Ahmad, Zeeshan; Kaario, Ossi; Qiang, Cheng; Larmi, Martti

Effect of negative valve overlap in a heavy-duty methanol-diesel dual-fuel engine : A pathway to improve efficiency

Published in:
Fuel

DOI:
10.1016/j.fuel.2022.123522

Published: 01/06/2022

Document Version
Publisher's PDF, also known as Version of record

Fuel 317 (2022) 123522

Contents lists available at ScienceDirect

Fuel

journal homepage: www.elsevier.com/locate/fuel

Full Length Article

Effect of negative valve overlap in a heavy-duty methanol-diesel dual-fuel engine: A pathway to improve efficiency

Zeeshan Ahmad *, Ossi Kaario, Cheng Qiang, Martti Larmi

Department of Mechanical Engineering, Aalto University, School of Engineering, 02150 Espoo, Finland

ARTICLE INFO

Keywords:
Methanol
Dual-fuel/RCCI
Negative-valve overlap
Exhaust emissions
EGR
High efficiency

ABSTRACT

Methanol (MeOH) is a promising low-carbon liquid fuel to provide global energy security with a potential to achieve net-zero greenhouse gas emissions in transport sector. However, its utilization in diesel engines at high MeOH substitution ratios (MSR) suffers from misfire or high pressure rise rates owing to its distinct physio-chemical properties. This issue is addressed in the present study by adopting negative-valve overlap (NVO) and hot residual gases from the previous cycle. Experiments are performed in a single-cylinder heavy-duty CI engine for a constant MSR (90% energy based) and an engine speed of 1500 rpm. The aim of the study is to investigate the effects of 1) NVO period, 2) charge-air temperature (T_{air}), 3) MeOH lambda (λ_{MeOH}) on the MeOH-diesel dual-fuel (DF) combustion in NVO mode, and 4) to demonstrate the implications of NVO in yielding high net-indicated efficiency (η_{ind}) together with low pollutant emissions at a wide range of engine operating loads (40–90%). The results show that the hot residual gases from the previous cycle enhance the reactivity of the fresh MeOH-air mixture by inducing slow oxidation processes before TDC_f. The slow pre-flame oxidation processes are disruptive or oscillatory in nature, wherein NVO period, T_{air} and λ_{MeOH} can be used to control these processes and their induced reactivity enhancing capability. It is noticed that the pre-flame oxidation processes and the main combustion have a direct correlation between them. Based on the control strategy, the MeOH-diesel combustion in the NVO mode produced on average η_{ind} of approx. 53% accompanied with very low NO_x emission of 1.1 g/kWh at a wide range of engine operating loads (40–90%). Additionally, on average the combustion phasing (CA50) is maintained at ~ 2 °CA aTDC, while the combustion stability remains high (COV_{IMEP} ~ 3.5%).

1. Introduction

EU's commitment to the global climate action under Paris agreement has led the governments to adopt ambitious targets to achieve net-zero greenhouse gas emissions by 2050 [1,2]. In this effort, where electrification of light-duty passenger vehicles is gaining its momentum [3,4], the plans of utilizing alternative- and renewable fuels in heavy-duty, marine, and power generation sectors with improved efficiency are also getting attention [5,6]. Methanol (MeOH), among many alternative fuels, is the simplest low-carbon and a clean burning fuel [7,8]. It can potentially contribute to achieve global net-zero emission targets when produced from biomass and the hydrogenation of atmospheric carbon dioxide (CO_2) using renewable energy sources [9,10]. Additionally, its single molecule morphology as a hydrogen carrier and the characteristic state of being liquid at standard conditions makes it a suitable transport fuel solution for storing and fuel transport infrastructure with minimal losses [7,10]. However, the efficient burning of MeOH in internal combustion engines (ICE) is one of the main challenges besides renewable MeOH supply that curbs its applicability. It is, therefore, important to further investigate and develop MeOH ICEs for improved efficiency and fuel consumption.

In the past, MeOH has been extensively studied in ICEs as a pure or blended fuel by many researchers [11–14]. In SI engines (dedicated MeOH or flex fueled M85 engines), it has been demonstrated to increase engine efficiency and power by 7–10% with lower unburned hydrocarbons (THC) and nitrogen oxides (NO_x) compared to counterpart gasoline engines [7,15]. MeOH leverages the benefits of octane boosting in SI engines, which enables the use of relatively high compression ratios and extends the limits of high-load engine operations. This allows the SI MeOH engines to achieve brake thermal efficiency (BTE) comparable to conventional diesel engines (~40%) [7,16]. However, the utilization of MeOH in diesel engines brings a distinctive set of challenges, which include extremely low cetane number and high heat of vaporization. In general, high-octane number indicates low cetane number. The cetane number of MeOH lies in the range of 2–3 [7,8,17], which makes its

* Corresponding author.
E-mail address: zeeshan.ahmad@aalto.fi (Z. Ahmad).

https://doi.org/10.1016/j.fuel.2022.123522
Received 11 October 2021; Received in revised form 11 January 2022; Accepted 4 February 2022
Available online 17 February 2022

Nomenclature

DF	Dual-fuel combustion
TDC_f	Firing top-dead center
TDC_{ex}	Exhaust top-dead center
^oCA aTDC	Crank angle degree after TDC
HRR	Apparent heat release rate
AccQ	Accumulative heat release
TFE	Total injected fuel energy
SVT	Standard valve timing
NVO	Negative valve overlap
MSR	Methanol substitution ratio
PMEP	Pumping mean effective pressure
n-, gIMEP	Net or gross indicated mean effective pressure
THC	Total unburned hydrocarbons
CO, CO_2	Carbon mono-, di-oxide
NO_x	Nitrogen oxides
$\dot{m}$	Mass flow rate
λ_{MeOH}	Methanol lambda
C_{input}	Total carbon content of injected fuel
η_{ind}	Net-indicated efficiency
η_{comb}	Combustion efficiency
η_{th}	Thermal efficiency
T_{air}	Charge air temperature
P_{air}	Charge air pressure
COV_{IMEP}	Coefficient of variations of gIMEP
SOI_{pilot}	Start of injection of pilot
SOI_{MeOH}	Start of injection of methanol
CA10, CA50, CA90	^oCA where 10%, 50%, and 90% of total heat releases
IVO, IVC	Intake valve opening, closing timing
EVO, EVC	Exhaust valve opening, closing timing
iEGR	Internal exhaust gas recirculation

autoignition difficult, particularly, when cylinder temperatures are also dropped due to latent heat of vaporization. In this scenario, combustion of MeOH in diesel engines requires either dedicated engines with high compression ratios [18] or advanced combustion technologies for existing diesel engines. Furthermore, there is more interest of improving diesel engines because heavy-duty applications typically employ diesel engines.

Dual-fuel (DF) is an advanced combustion concept, which uses two fuels of different reactivities [19–21]. Typical examples of DF engines are already available in the market in which the DF concept is realized either by adopting port-fuel injection (PFI), direct injection (DI) or reactivity-controlled compression ignition (RCCI) combustion technologies. In MeOH-diesel DF combustion, MeOH is ignited by pilot diesel close to the top-dead center. Wang Q. et al. [22] investigated MeOH-diesel PFI-DF combustion at varying engine loads (6% to 100%) with various MeOH substitution ratios (MSR). Only at medium loads, they could use a maximum MSR of 76%. They reported a restriction in using such high MSR at low or high loads due to partial burn, misfire, or knocking combustion. They concluded that the maximum employable MSR is quite load dependent. On the other hand, in all their experiments, they showed BTE below 38%. In a later publication, Wang B. et al. [23] attempted to further explore high-load (75% and 100%) engine operations by employing exhaust-gas recirculation (EGR) and controlled pilot injection timings at various MSR. They utilized maximum MSR of 80%. The results depicted a misfire occurrence at 1660 rpm when using MSR beyond 80% with 17% EGR. However, they reported a significant reduction in NO_x and soot emissions with high MSR, nonetheless, also with high emissions of THC and carbon monoxide (CO). Similarly, Tutak et al. [24] investigated MeOH-diesel PFI-DF combustion at varying loads with various MSR, where they could employ maximum MSR of 90% only at full load (24 kW). They also reported a reduction in NO_x and soot emissions, however, with an increase in THC and CO at increasing MSR. They reported BTE below 35% where at part loads (16 kW and 8 kW), combustion efficiency was demonstrated to drop drastically with increasing MSR.

RCCI-DF combustion (either PFI or DI mode of MeOH) allows an explicit control of mixture's in-cylinder reactivity stratification by adopting various fuel injection strategies. This is generally considered an advantageous procedure for improving combustion efficiency together with low NO_x and soot emissions [25–28]. Duraisamy et al. [29] studied single pilot (SOI = -10 CA ATDC) MeOH-diesel PFI-RCCI combustion to explore the effects of MSR and hot/cold EGR. They used two engine loads with maximum 90% MSR only at high load. They summarized the study with similar conclusions as above. That is, with increasing MSR, NO_x and soot emissions reduce with increasing emissions of THC and CO. Also, cooled EGR is more beneficial than hot EGR for improving efficiency. Nevertheless, in their experiments, they reported maximum BTE < 35%. Jia et al. [30] performed a comparative RCCI (split diesel injection) study at varying loads with 50–76% MSR for three different MeOH injection strategies i.e., PFI, DI during the intake stroke, and DI during the compression stroke. They also employed EGR with optimized injection timings to control combustion for the best possible efficiency gains. In their experiments, a maximum indicated efficiency<48% is reported. However, they concluded that the PFI strategy is more efficient than the DI strategies, which also maintains ultra-low NO_x and soot at high loads.

Recently, Huang et al. [31] investigated the same RCCI-DI MeOH strategy with split diesel injection for varying MSR in a range of 30–60%. They called this mode as intelligent-charge compression ignition (ICCI) combustion whereby they realized high efficiency and low emissions. All presented results at IMEP = 8 bar show indicated efficiency below 48% together with low NO_x emissions, however, with rather high THC and CO emissions. Nevertheless, they reported high indicated efficiency of 53.5% only at IMEP = 12 bar using 50% MSR. Apart from this, Dong et al. [32] studied non-premixed DI-DF combustion at varying loads with various MSR in the range of 40–95%. They reported an improved indicated efficiency and combustion stability with increasing load and MSR together with decreased CO and THC emissions. However, in this study, the maximum indicated efficiency was attained<45% for a full range of experiments. Also, the burning of 100% MeOH in DI-PPC mode produced indicated efficiency below 45% [33].

Based on the above literature and other review articles [7,8,34], it is apparent that using high MSR is more desirable to achieve net-zero emission targets at a wide range of engine operations. However, the phenomenon like misfire or high pressure-rise rates limits its applicability. Moreover, high MSRs are suggested to be favorable only for optimized high-load engine operations with maximum achievable indicated efficiency<50%. Therefore, in this study, we attempt to investigate diesel-methanol PFI-DF combustion in a single-cylinder heavy-duty engine using a constant MSR of 90%. For this purpose, we utilize an internal EGR (iEGR) strategy with its counteracting effects of high temperature and dilution using negative-valve overlap (NVO).

NVO is a well-known variable-valve actuation (VVA) strategy for improving lean operations of a single fuel type HCCI combustion concepts [35,36]. However, it has been scarcely reported for DF combustion. Only few studies [37–39] have used NVO in DF concept with an aim to improve low-load engine operations by leveraging fuel reforming [37,38] with an additional fuel injection at the end of the exhaust stroke. In this study, we address this significant research gap by investigating the PFI-DF combustion in NVO mode, however, without any additional

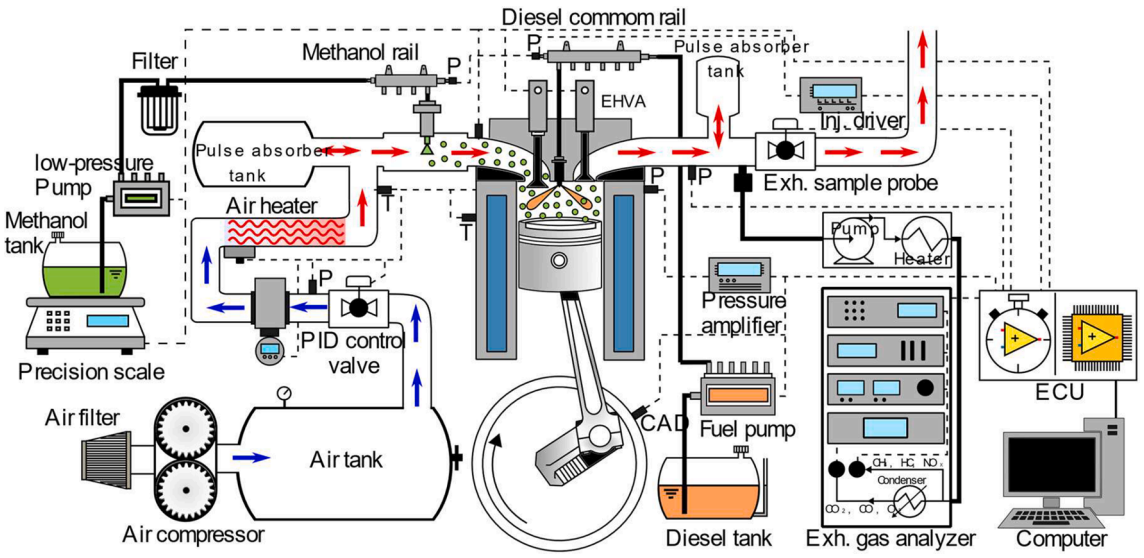

Fig. 1. A schematic diagram of the research engine setup.

Table 1
Research engine specification [20,40].

Engine type	4 Stroke, modified single-cylinder DF engine
Piston geometry	Re-entrant bowl
Displacement volume	1.4 L
Bore × Stroke	111 × 145 mm
Geo. compression ratio	16.7:1
No. of valves	4
In-cylinder swirl ratio	2.7 [42]
Pilot injection system	Bosch common rail with piezoelectric injector
Injector no. of holes × diameter	3 × 0.160 mm (symmetric)
Port-fuel injection system	1 × Bosch methanol injector
Firing TDC (TDC_f)	0 °CA aTDC
Gas exchange TDC (TDC_{ex})	360 °CA aTDC

Table 2
Description of exhaust gas analyzers [40].

Emission type	Analyzer and measuring principle	Measuring range	Measurement Uncertainty
THC	A heated-flame ionization detection (HFID) based analyzer Model VE-7 (J.U.M Engineering GmbH)	0–3000 ppm	<30 ppm[a]<45 ppm[b]
CO, CO_2	SIDOR non-dispersive infrared spectroscopy (NDIR) based analyzer (Sick AG)	CO: 0 – 3000 ppm, CO_2: 0 – 30 vol%	CO: ±3 ppm, CO_2: <0.05 vol%
O_2	A paramagnetic dumbbell (OXOR-P) analyzer (Sick AG)	0–25 vol%	<0.05 vol%
NO, NO_2, NO_x	CLD-822Sh (ECO Physics AG) analyzer based on chemiluminescence	NO_x: 0 – 2000 ppm	<20 ppm

[a] for non-oxygen species.
[b] for oxygen containing species.

fuel injection. In addition, we employ a one-dimensional (1D) GT-power based engine model to estimate iEGR percentage and in-cylinder mixture temperatures. Thus, this study aims to:

1) fundamentally investigate the MeOH-diesel DF combustion in NVO mode at varying a) NVO period, b) charge-air temperature, and c) MeOH lambda,

2) demonstrate the ability of the DF combustion in NVO mode to achieve high net-indicated efficiency ($\eta_{ind} \sim 50\%$), together with ultra-low exhaust emissions at varying engine loads (40–90%) with a constant MSR of 90%.

2. Experimental setup and methods

2.1. Research engine setup

Like our previous studies [20,40], a compression ignition (CI) single-cylinder heavy-duty engine is used here as a DF research engine. Fig. 1 shows a schematic of the laboratory engine setup. The specifications of the research engine are outlined in Table 1. The engine is equipped with necessary auxiliary systems and several monitoring devices to flexibly control engine parameters. A 45 kW process performance electric motor coupled with a frequency converter handles the load and desired engine speed. Of special importance to the present study, an electro-hydraulic-valve-actuation (EHVA) [41] hardware operates the valve train with variable-valve timings and lifts. Hence, with EHVA, various VVA strategies including NVO can be controlled in a flexible manner while running the engine.

A PID-based charge-air system supply fresh air into the engine. It consists of a compressor, air-heater, control valve, and RHM-08 Coriolis mass-flow meter (Rheonik Messtechnik GmbH, Accuracy < 0.1% of flow [40]) controlling the desired pressure, temperature, and mass-flow rate of the fresh air. Similarly, a port-fuel injection system consisting of a low-pressure pump, fuel-cooling system, weighing scale (Accuracy < 0.5 mg) and a port-fuel injector (Bosch, GmbH) delivers a desired mass of MeOH into the cylinder at a desired injection timing. On the other hand, a piezo injector directly delivers diesel pilot into the cylinder with an ability to control injection timing and duration [20,40]. In addition, the engine is equipped with an in-cylinder pressure sensor (Kistler 6125C) and a charge amplifier (Kistler 5011b) to measure pressure inside the cylinder at a resolution of 0.2 crank angles.

The engine is provided with exhaust-gas analyzing system containing various emission analyzers for measuring THC, CO, CO_2, oxygen (O_2) and NO_x. A suction pump extracts a sample of raw emission gases from the exhaust runner via a heated probe and delivers it to the analyzers. The details of the analyzers are summarized in Table 2 [40]. An engine control unit monitors all devices and auxiliary systems, which also enables a high-speed data acquisition at 40 MHz and a flexible control of engine operating parameters.

2.2. Test fuels

In the present study, 99.9% pure MeOH and commercial diesel complying with the European EN590 standard are employed as the test fuels. MeOH is utilized as the main fuel, which is a simple low-carbon

Table 3
Test fuels specifications; EN590 [43], Methanol [44,45].

Properties	Diesel (EN590)	Methanol
Molecular formula	$C_{12} - C_{20}$	CH_3OH (MeOH)
Cetane number	≥ 51.0	2–3
Density [kg/m^3] at 20 °C	820–845	791
Viscosity [mm^2/s] at 40 °C	2–4.5	0.56
Boiling point [°C]	200–360	65
Lower heating value [MJ/kg]	43.2	19.9
Energy density [MJ/m^3]	35260–36335	15503
Standard heat of vaporization [kJ/kg]	225–280	1165
Auto-ignition temperature [°C]	230	464
Heat capacity ratio ($\gamma = c_p/c_v$) at 77 °C	–	1.203
C-content [wt. %]	86.5	37.48
H-content [wt. %]	13.5	12.58
O-content [wt. %]	0	49.93
Water content [wt. %]	<0.02	<0.01
Air-to-fuel ratio	14.7	6.47

liquid fuel with a boiling point of 65 °C. However, it's high latent heat of vaporization establishing a challenge for a reliable combustion in CI engines. Additionally, it's extremely low cetane number and high auto-ignition temperature add up a difficulty to its ignition. Therefore, diesel is used as the pilot fuel to ignite the premixed MeOH-air mixture close to the top-dead center (TDC_f). The properties of the test fuels are listed in Table 3.

2.3. Operating conditions and procedure

In this study, experiments are carried out at a constant engine speed of 1500 rpm in the NVO mode. Fig. 2 illustrates the concept of NVO using a representative cylinder pressure, intake, and exhaust valves. The NVO is attained by closing the exhaust valve earlier and opening the intake valve later than the gas-exchange TDC (TDC_{ex}). Thus, NVO represents a crank-angle period between exhaust-valve closing (EVC) and intake-valve opening (IVO) timings. Table 4 outlines the valve timings and other constant operating conditions. With NVO, a fraction of exhaust gases is trapped inside the cylinder, which is referred as residual gases. These gases undergo a re-compression and -expansion process around the TDC_{ex} (see Fig. 2). Later during the intake stroke, the intake valve opens at 420 °CA aTDC delayed enough to avoid any backpressure into the intake port. Meanwhile, methanol is port injected at SOI_{MeOH} = 420 °CA aTDC and supplied into the cylinder along with fresh air as soon as the intake valve opens. The fresh MeOH-air charge may experience pre-combustion processes during the early cycle due to the presence of high-temperature residual gases from the previous cycle. Later at the end of the compression stroke, diesel pilot is injected at SOI_{pilot} = -6 °CA aTDC to ignite the premixed MeOH-air mixture close to TDC_f.

It should be noted that in this study the period of NVO is varied by sweeping the EVC timing. As EVC timing advances with respect to TDC_{ex}, the period length increases, and vice versa. The employed EVC sweeps along with representative EVC are presented in Fig. 2. On the other hand, during experiments a constant fraction i.e., 90% of total-fuel energy (TFE) is supplied by MeOH, whereas only 10% (TFE based) diesel is utilized as pilot to ignite the MeOH-air mixture. In addition, charge-air mass flow (m_{air}), temperature (T_{air}), and boost pressure (P_{air}) are adjusted according to the experimental test matrix, as described in Section 2.4. Furthermore, as a pre-engine-run condition, the engine cooling water is heated up to 70 °C via external water heating system to evenly heat up the engine block, cylinder head and the liner. The test fuels are injected only after achieving the stable initial operating conditions.

After injecting test fuels, the engine is continuously run for 5 min in order to record the test data reliably including the averaged exhaust emissions data. Total hydrocarbons (THC) including oxygenated components (e.g., derivatives of aldehydes, mainly formaldehyde) produced from incomplete combustion of MeOH are measured by flame-ionization detection (FID) based analyzer. It should be noted that FID analyzer is calibrated with propane (non-oxygenated fuel), which may induce uncertainty in the measurements. Additionally, FID technique offers lower sensitivity for oxygenated hydrocarbons compared to non-oxygenated hydrocarbons [46]. Regardless, this systematic uncertainty in

Table 4
Constant operating conditions.

Engine speed [rpm]	1500
Pilot injection pressure [bar]	1000
MeOH substitution ratio (MSR)	90%
MeOH injection timing (SOI_{MeOH})	420 °CA aTDC
Pilot ratio (P_R)	10%
Pilot injection timing (SOI_{pilot})	−6 °CA aTDC
Intake valve opening (IVO)	420 °CA aTDC
Intake valve closing (IVC)	−155 °CA aTDC
Exhaust valve opening (EVO)	150 °CA aTDC
Exhaust valve closing (EVC)	265 – 320 °CA aTDC

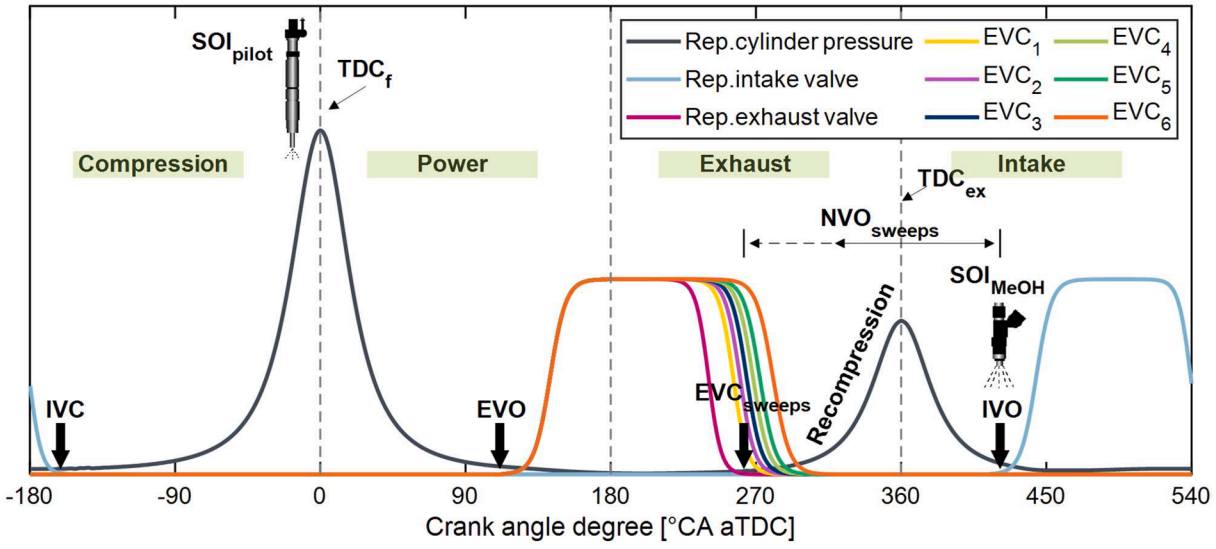

Fig. 2. A schematic concept description of negative valve overlap (NVO) and sweeps of exhaust valve closing (EVC) timing. NVO represents a crank-angle period between EVC and IVO. For a comparison, the baseline standard valve timing (SVT) is presented in Fig. A1 in Appendix A.

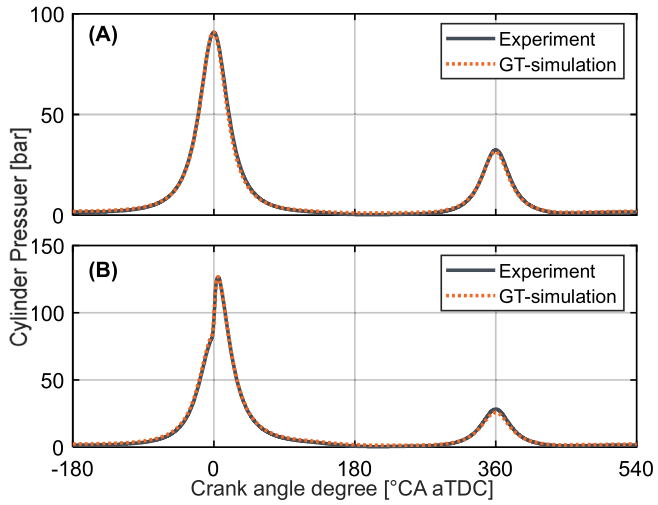

Fig. 3. Validation of (A) 1D GT-power engine model for intake and exhaust gas dynamics (motored case) in NVO mode at measured initial conditions, (B) full cycle Three Pressure Analysis (TPA) method for estimation of thermodynamic in-cylinder conditions of the studied MeOH-diesel DF combustion case. Here, all the imposed (measured) conditions are the same for (A) and (B).

measurement is<1.5% of the full scale (for oxygenated fuels), as mentioned in Table 2. Apart from this, in this study, the concentration of raw exhaust emissions measured in parts per million by volume (ppm) is converted to (gross) indicated specific emissions (g/kWh) based on stoichiometry [47]. In conversion calculations, the molecular weight of total hydrocarbon is adjusted for oxygen part so that 50% higher mass of total hydrocarbons are estimated (since 2009, EU regulation on the certification of flex fuel vehicle driven on E85 [48]).

In the present study, in-cylinder pressure data for 200 successive combustion cycles is recorded and averaged for each test point. The undesired noise from raw-pressure data is filtered by using a low-pass Butterworth filter algorithm [20,40]. The cylinder pressure data is then used to calculate apparent heat release rate (HRR) and accumulative heat release (AccQ) based on the first law of thermodynamics using Equations 1 and 2. Additionally, net- and gross-indicated mean effective pressures (nIMEP, gIMEP) are calculated for intervals −180 to 540 and −180 to 180, respectively [20,40]. The pumping mean effective pressure (PMEP) is calculated as a difference between nIMEP and gIMEP. Here, combustion stability is determined by the coefficient of variability of gIMEP (COV_{IMEP}), which is estimated using the standard deviation method. Other important performance parameters such as MeOH lambda (λ_{MeOH}), total-fuel energy (TFE), combustion efficiency (η_{comb}), net-indicated efficiency (η_{ind}) and thermal efficiency (η_{th}) are calculated according to Equations (3) to (7).

$$HRR = \frac{dQ}{d\theta} = \frac{\gamma}{\gamma-1}P\frac{dV}{d\theta} + \frac{1}{\gamma-1}V\frac{dP}{d\theta} \tag{1}$$

$$AccQ = \int \frac{dQ}{d\theta}d\theta \tag{2}$$

$$\lambda_{MeOH} = \frac{\left(\dot{m}_{air}/\dot{m}_{MeOH}\right)_{actual}}{(AFR_{MeOH})_{stoichiometric}} \tag{3}$$

$$TFE = LHV_{MeOH} \times \dot{m}_{MeOH} + LHV_{diesel} \times \dot{m}_{diesel} \tag{4}$$

$$\eta_{comb} = \frac{CO_2}{TotalC_{input}} \times 100 \tag{5}$$

$$\eta_{ind} = \frac{nIMEP \times V_{displacement}}{TFE} \times 100 \tag{6}$$

$$\eta_{th} = \frac{gIMEP \times V_{displacement}}{\eta_{comb} \times TFE} \times 100 \tag{7}$$

2.3.1. 1D GT power simulations

A 1D engine model based on GT-power by Gamma technologies is used here to mainly estimate the amount of trapped residual gases and mean mixture temperatures for the DF combustion in NVO mode. First, an engine model was developed for the single-cylinder research engine

Table 5
Experimental test matrix and corresponding performance parameters.

Test point	EVC type	$\dot{m}_{PF}$ [mg/cycle]	$\dot{m}_{MeOH}$ [mg/cycle]	TFE [J/cycle]	P_{air} [bar]	T_{air} [°C]	λ_{MeOH}	nIMEP [bar]	gIMEP [bar]	PMEP [bar]	η_{comb} [%]	η_{ind} [%]	η_{th} [%]
	Comparison of NVO and SVT												
SVT	EVC_{rep}	4.66	77.77	1750	1.15	40	3	1.88	2.1	−0.22	33.20*	15.07	50.70
NVO	EVC_{rep}	4.66	77.77	1750	2.01	40	3	6.47	6.41	0.06	93.20*	51.87	55.15
	Effect of Negative Valve Overlap period												
NVO120	EVC4	4.44	90.44	1992	1.92	40	3.4	6.43	6.31	0.12	85.90*	45.28	51.75
NVO125	EVC3	4.44	90.44	1992	2.00	40	3.4	7.34	7.22	0.12	94.78*	51.71	53.65
NVO130	EVC2	4.44	90.44	1992	2.07	40	3.4	7.52	7.37	0.15	92.50	52.99	56.13
NVO135	EVC1	4.44	90.44	1992	2.15	40	3.4	7.65	7.48	0.17	94.60	53.86	55.70
	Effect of Charge-air Temperature												
CAT40	EVC2	4.44	90.44	1992	2.28	40	3.8	7.24	7.05	0.19	94.44*	50.97	52.58
CAT50	EVC2	4.44	90.44	1992	2.32	50	3.8	7.60	7.40	0.20	97.57*	53.55	53.42
CAT60	EVC2	4.44	90.44	1992	2.38	60	3.8	7.65	7.42	0.23	94.56	53.91	55.30
CAT70	EVC2	4.44	90.44	1992	2.43	70	3.8	7.67	7.40	0.27	96.40	53.99	54.10
	Effect of MeOH Lambda												
ML32	EVC2	4.44	90.44	1992	1.95	40	3.20	7.51	7.40	0.11	95.07	52.91	54.82
ML34	EVC2	4.44	90.44	1992	2.05	40	3.40	7.48	7.33	0.15	95.51*	52.68	54.05
ML36	EVC2	4.44	90.44	1992	2.15	40	3.60	7.38	7.21	0.17	95.41*	52.00	53.23
ML38	EVC2	4.44	90.44	1992	2.25	40	3.80	7.11	6.90	0.21	92.80*	50.05	52.37
	Effect of Engine Loads												
EL40	EVC6	4.44	61.3	1413	1.54	100	4.0	4.98	4.96	0.02	95.06	49.46	51.82
EL50	EVC6	4.44	72.7	1638	1.48	80	3.3	5.94	5.92	0.02	95.98	50.87	52.82
EL60	EVC3	4.44	88.9	1961	2.08	50	3.5	7.56	7.44	0.12	94.89	54.10	56.09
EL70	EVC3	5.55	106.7	2363	2.01	40	2.9	8.95	8.8	0.15	97.03	53.16	53.85
EL80	EVC5	6.22	119.5	2648	2.10	50	2.9	9.97	9.85	0.12	97.37	52.84	53.59
EL90	EVC6	7.33	132.2	2948	1.95	50	2.6	10.72	10.7	0.02	97.5	51.01	52.22

* Calculated using $\eta_{comb} = AccQ/TFE \times 100$, because CO emission analyzer was saturated. We found that η_{comb} calculated using Equation (5) are usually 2–5% lower than this method depending on CO emission level.

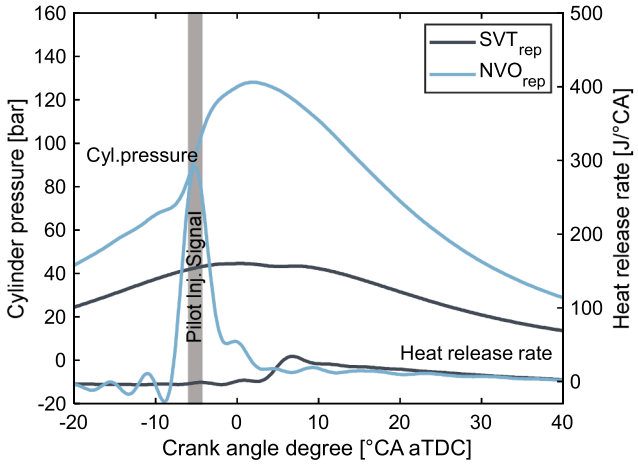

Fig. 4. Cylinder pressure and heat release rate data for comparison of SVT and NVO. The representative valve timings for SVT and NVO are illustrated in Fig. 2 and Fig. A1, respectively.

with all possible components including piping, tanks, valves, and ports. Fig. 3(A) shows the validation of the engine model against motored (no fuel) cylinder pressure at the measured initial conditions. This represents an adequately calibrated engine model for the intake and exhaust gas dynamics.

Later, the model was further developed based on the full cycle, Three Pressure Analysis (TPA) [49] method and introduced with DF fuel injection systems. The TPA method uses the measured cylinder pressure data to calculate apparent burn rate and imposes it to the simulation cycle for the combustion prediction. TPA is an iterative method until the simulated cylinder pressure matches the measured one. Fig. 3(B) shows the validation of the TPA method with the experimental cylinder pressure data of MeOH-diesel DF combustion. It should be noted that the engine conditions for Fig. 3(A) and (B) are the same. On the other hand, measured emissions of THC (C1 carbon based), CO and NO are imposed in the combustion model to estimate η_{comb}. However, 1D model-based η_{comb} is used only for validation purposes, where we observed an error of<2% for all studied cases. Furthermore, the percentage of iEGR is defined as the ratio of the trapped mass of residuals ($m_{residual}$) to the total mass of mixture inside the cylinder (m_{total}), according to Equation 8.

$$\text{iEGR} = \frac{m_{residual}}{m_{total}} \times 100 \tag{8}$$

2.4. Test matrix

This study aims to investigate the characteristics of MeOH-diesel DF combustion in the NVO mode, and to demonstrate the ability to control a wide range of engine operating loads with an adequate combustion stability, improved emissions, and positive efficiency gains. However, first we compare NVO with standard-valve timing (SVT) briefly to emphasize the benefits of using NVO mode. Then, to proceed with the NVO mode investigation, the experimental test matrix is categorized in four test cases as, 1) effect of negative-valve overlap (NVO) period, 2) effect of charge-air temperature (CAT), 3) effect to methanol lambda (ML), and 4) effect of varying engine load (EL). The experimental test points and corresponding performance parameters are summarized in Table 5. Here, all experiments are performed under design-of-experiment approach to achieve $\eta_{comb} \geqslant 90\%$.

In each test case, the corresponding test points are identified from their characteristic name. For example, NVO120 indicates a test point with NVO period of length 120 °CA and so on. Similarly, CAT40, ML32, and EL40 represent the test points of charge-air temperature of 40 °C, methanol lambda of 3.2, and engine load of 40%, respectively. It should be noted that here engine load is defined as a ratio of 90% of the TFE to the maximum rated engine power per cylinder. The test cases #1–3 are performed for constant operating parameters except for the parameter under investigation. However, in the test case of engine load variations, all parameters are adjusted to achieve engine performance results above a set threshold. These thresholds include 1) CA50 ≈ 2 °CA aTDC, 2) $\eta_{comb} \geqslant 90\%$, 3) $\eta_{ind} \sim 50\%$, and 4) $\text{COV}_{\text{IMEP}} < 5\%$.

3. Results and discussion

3.1. Comparison of NVO and SVT

Prior to the detailed investigation, MeOH-diesel DF combustion is compared here using two different valve configurations at constant operating conditions, as listed in Table 5. SOI_{MeOH} is adjusted according to the corresponding IVO timing. The compared NVO and SVT configurations, labelled as representative intake and exhaust valves, are illustrated in Fig. 2 and Fig. A1, respectively. The obtained results of cylinder pressure and HRR are presented in Fig. 4. The combustion with NVO is observed to produce significantly higher cylinder pressure and HRR compared to SVT. Also, NVO assists producing higher η_{comb} of 93% compared to 33% as produced with SVT. Despite the constant conditions, the reason for attaining such high efficiency with NVO may be associated with implicitly higher compression pressure, temperature and internal EGR (iEGR). Therefore, for validation, additional experiments were performed to investigate the combustion with SVT at increased boost pressure ($P_{air} \sim 2$ bar) and charge-air temperature ($T_{air} \sim 150$°C), while keeping other conditions constant. For brevity, the

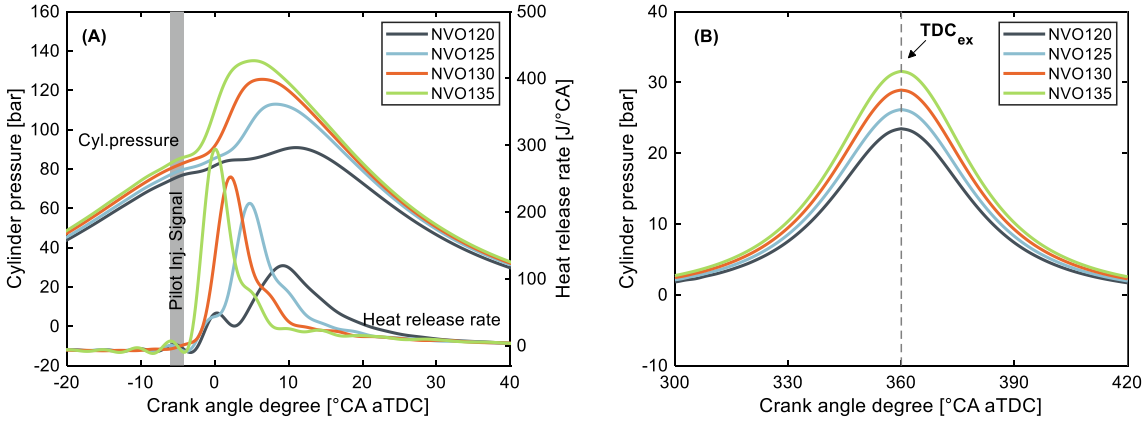

Fig. 5. (A) Cylinder pressure and heat release rate around TDC_{f}, and (B) only cylinder pressure around TDC_{ex} at varying NVO period.

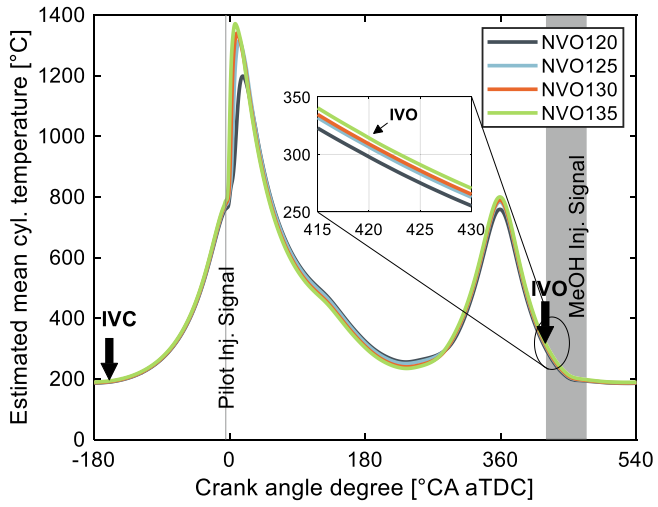

Fig. 6. Simulated mean cylinder temperatures using GT power TPA method for test points NVO120 to NVO 135.

results are not presented here, nevertheless, the η_{comb} was observed to improve to approx. 80%. However, the early start of combustion and its phasing were unrealistic. The use of cold EGR could be advantageous for controlling the phasing of the start of combustion.

In an attempt to improve the combustion with SVT, it is also found that SOI_{pilot} earlier than −12 °CA aTDC (RCCI mode at 90% MeOH) is unfavorable at such high temperatures. Moreover, the implementation of the split injection strategy is restricted due to the small pilot quantity (10%) and the operational limits of the injector. In brief, compared to NVO, the combustion with SVT requires drastically high charge-air temperatures and a complex control of parameters to reliably attain $\eta_{comb} \geqslant 90\%$. Therefore, in this study, 10/90 diesel-methanol DF combustion is investigated and controlled at varying loads using NVO method. In addition, in this way part of waste heat from exhaust gases can be recovered.

Here, it should be noted that in this study NVO method is used as a combination of early EVC together with late IVO timing, which is considerably more efficient VVA strategy compared to using early EVC timing alone. With late IVO, most of the work spent on the re-compression of the residual gases can be recovered during the re-expansion process, while only some of the work is lost (pumping loss) as heat transfer to the cylinder walls. In this study, moderate levels of boost pressures (1.5 – 2.0 bar) are also utilized, which compensates the lost work and influences the nIMEP positively, as shown in Table 5. More details about the potentials of NVO compared to various VVA strategies (including PVO) can be found in a publication by Rodriguez J.F. et al. [50].

3.2. Effect of NVO period

The period of NVO regulates the amount of residual gases trapped inside the cylinder. In this study, it is controlled by varying EVC timing, as described in Section 2.3. To understand the effect of trapped residual gases, the combustion is investigated at four various NVO periods under constant operating conditions, as outlined in Table 5. The obtained results of cylinder pressure and HRR for test points NVO120-NVO135 are presented in Fig. 5. The combustion improves with an increase in the residual gas amount. It can be observed that the peak cylinder pressure and peak HRR increases as NVO period prolongs from NVO120 to NVO135. A greater amount of hot-residual gases retains inside the cylinder when the NVO period is extended. Consequently, the retained residual-gas mass enhances the in-cylinder thermodynamic state. Fig. 6 presents mean mixture temperatures for the studied test points, as estimated using the GT-power based TPA method explained in Section 2.3.1.

It can be observed that trapped mass of residual gases has a pronounced effect on the simulated mean mixture temperatures. In the re-compression and -expansion process around TDC_{ex}, the peak temperature increases by ~ 40 °C between NVO120 and NVO135, which is roughly a gain of ~ 5%. This thermal gain nevertheless sustains also during the intake stroke, although the temperature ranges are lower. Interestingly, at IVC timing, the simulated mean mixture temperature retains at ~ 190 °C despite the latent heat absorbed by MeOH during the early intake stroke (after IVO). It is estimated that at IVO timing, fresh MeOH is injected into bulk ambient temperature of ~ 300–320 °C, which gradually drops to ~ 185–195 °C (at IVC). Here, it is interesting to note that such a thermodynamic state facilitates the thermal cracking or slow partial oxidation of the fresh MeOH in the presence of residual gases, which may lead to the production of reactive species and thus to earlier autoignition of the in-cylinder mixture.

Aniolek et al. [51] investigated such slow oxidation of methanol at similar temperature and pressure conditions in a constant volume stirred reactor. They reported that HO_2 is the active specie that leads to $CH_3OH \rightarrow CH_2OH \rightarrow CH_2O \rightarrow CHO \rightarrow CO$ as a result of partial oxidation of MeOH in the pre-flame regime. However, they also reported a heterogeneous termination of HO_2 chain branching at low temperature and pressure (below 650 K at 700 torr or here below 200 °C at 1.5 bar). This is, however, less important at elevated conditions during compression stroke or close to TDC_f when the in-cylinder mixture temperature rises to an autoignition trigger point or pilot diesel is injected. At high temperatures, HO_2 enhances the production of OH radicals via direct dissociation of H_2O_2 that initiates high temperature (main) combustion around TDC_f.

In summary, the high temperatures (300–320 °C) during MeOH in-

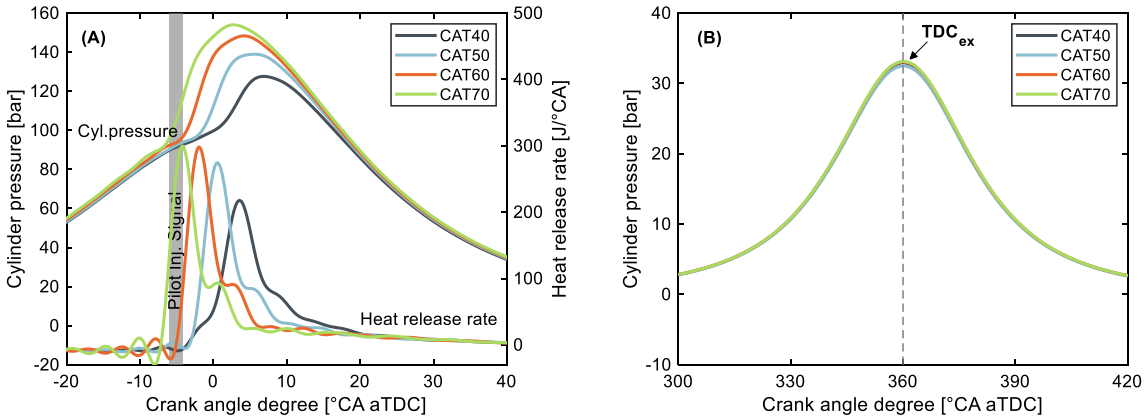

Fig. 7. (A) Cylinder pressure and heat release rate around TDC_f, and (B) only cylinder pressure around TDC_{ex} at varying T_{air}.

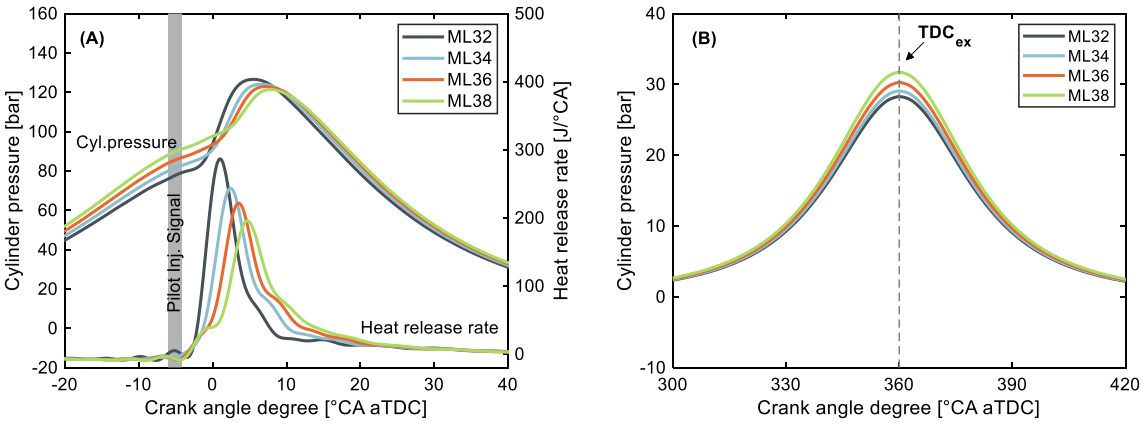

Fig. 8. (A) Cylinder pressure and heat release rate around TDC_f, and (B) only cylinder pressure around TDC_{ex} at varying λ_{MeOH}.

jection together with residual gases are the main reason for improving MeOH-diesel DF combustion. Whereby, NVO period depicts a direct influence on the autoignition of the in-cylinder mixture due to reactive species generated during slow oxidation in the pre-flame regime. Thus, after analyzing several performance parameters (not presented here for brevity), we observe that with an increase in the NVO period, the combustion phasing (CA10, CA50, and CA90) advances, AccQ, gIMEP, η_{ind} and η_{comb} are increasing (see Table 5). Additionally, THC and CO emissions are reduced significantly.

3.3. Effect of charge-air temperature (T_{air})

Next, we demonstrate the impact of T_{air} on the performance of MeOH-diesel DF combustion in the NVO mode. It is worth noting that the investigation at richer conditions is limited by high pressure-rise rates, early autoignition and strong acoustic oscillations. In addition, the combustion at richer conditions is found to be highly sensitive to T_{air}. Therefore, a leaner condition ($\lambda_{MeOH} = 3.8$) is selected here and only T_{air} is varied, while keeping other operating conditions constant, as outlined in Table 5. In this case study, several performance parameters and emission characteristics are analyzed, however, for brevity only the relevant cylinder pressure and HRR data is presented in Fig. 7.

Temperature is an important parameter for determining the Arrhenius rate of chemical reactions. In general, high temperatures accelerate the rates of combustion by increasing the kinetic energy and collision probability of the fuel/oxidizer molecules within a mixture. Thus, high temperatures can be advantageous for the pre-flame slow oxidation and promoting the autoignition of the main combustion. It is observed from Fig. 7(A) that the peak cylinder pressure and peak HRR increase with the increase in T_{air} from CAT40 to CAT70. In particular, the pre-flame slow oxidation processes (reactivity) are enhancing from CAT40 to CAT70 and producing a larger amount of reactive species (as discussed in Section 3.2). Whereby these promote early autoignition of the MeOH-air mixture at respectively higher compression temperatures. As an evidence, CAT60 and CAT70 depict autoignition even earlier than pilot diesel injection timing. Nevertheless, CO emissions decrease because of completed combustion with monotonically higher exhaust-gas temperatures. The increased temperature of residual gases has also a pronounced effect of promoting the slow pre-flame oxidation processes before ignition occurs.

In this case, the main-combustion duration (interval between CA2 and CA90) is found to increase ~ 2 °CA per 10 °C increase in the T_{air} although the start of combustion (~CA2) also advances ~ 2 °CA per 10 °C. This particular behavior is attributed to 1) a faster burning rate during the early stage of the main combustion and 2) slow burning during the late cycle because of dilution induced by greater fuel burned in early main-combustion stages. On the other hand, we observe that gIMEP increases with the increase in T_{air} from CAT40 to CAT50, however, for CAT60 to CAT70 gIMEP remains unchanged (see Table 5). This is due to early combustion phasing with respect to TDC_f and negative work produced.

In brief, increased T_{air} enhances the reactivity or pre-flame slow oxidation processes, which consequently promotes autoignition and improves the overall combustion. We found that at the lean condition, increased T_{air} advances the combustion phasing (CA10 and CA50, however, delays CA90), helps to increase AccQ, gIMEP, η_{ind} and η_{comb} accompanied with significantly reduced THC and CO emissions.

3.4. Effect of MeOH lambda (λ_{MeOH})

Relative air/fuel ratio is one important parameter for characterizing combustion. It indicates the quality of air-to-fuel mixture, particularly, the flammability and reactivity stratification of the in-cylinder mixture. To understand how relative air/fuel ratio affects the performance of MeOH-diesel DF combustion in the NVO mode, the experiments (ML32 - ML38) are performed for constant operating conditions at varying λ_{MeOH}, as listed in Table 5. It should be noted that λ_{MeOH} is increased by increasing P_{air}, which correspondingly increases the charge-air quantity. For brevity, only the relevant results of cylinder pressure and HRR are presented in Fig. 8.

It can be seen from Fig. 8(A) that as λ_{MeOH} increases from ML32 to ML38, the peak cylinder pressure and peak HRR decrease although the compression pressure increases. This may be due to over-lean mixtures, which subsequently leads to an incomplete combustion, a reduced combustion efficiency and lower exhaust-gas (or residual gas) temperature. For instance, the measured exhaust gas temperature decreases from 235 °C to 195 °C when λ_{MeOH} is increased from 3.2 to 3.8. However, here it is interesting to note that despite the respective lean mixtures, the start of combustion timing (~CA2) is maintained from ML32 to ML38. This may be attributed to increased amount of reactive species produced during the pre-flame slow oxidation processes with the increased λ_{MeOH} value.

For the same NVO period, increased boost pressure (increased λ_{MeOH}) leads to retain a greater amount of residual gases inside the cylinder. As noted in Section 3.2, for the constant λ_{MeOH}, the increased residual gases enhance the reactivity of the fresh MeOH-air mixture as a result of pre-flame slow oxidation processes with increasing exhaust-gas temperatures. Likewise, here at varying λ_{MeOH}, the increased residual gases enhance the reactivity however, with decreasing exhaust-gas temperatures. This indicates that the composition of exhaust-gases is also an important factor influencing the ignition timing and determining the characteristics of the pre-flame slow oxidation. However, despite the maintained start of combustion timing, over-lean mixtures (or dilution) prevail around TDC_f (while MeOH is being injected during the intake stroke, the mixture is rather heterogeneous than homogenous) and worsen the main combustion (reduced η_{comb}) as λ_{MeOH} increases from

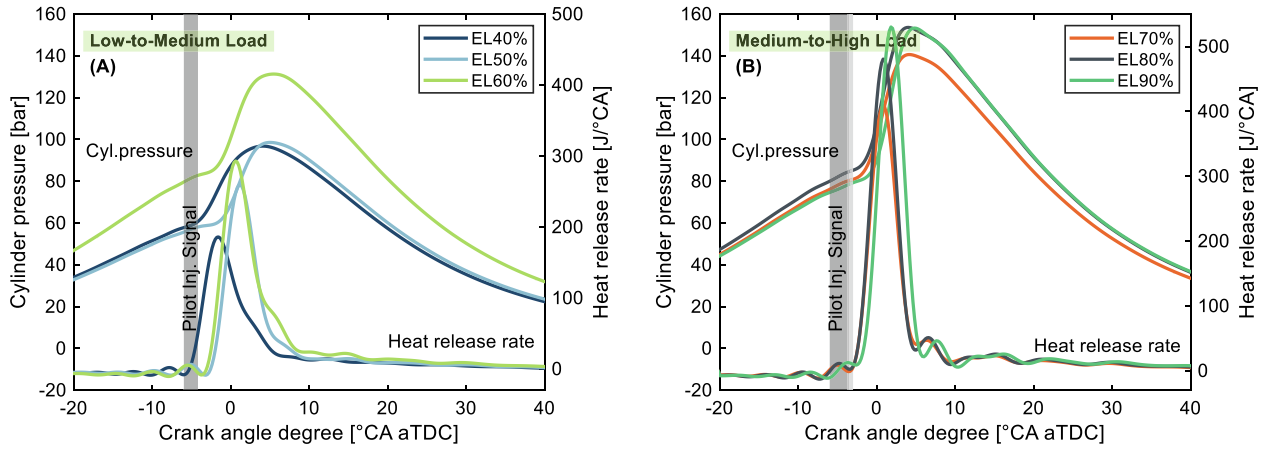

Fig. 9. Cylinder pressure and heat release rate at varying engine loads, (A) Low to medium loads, (B) Medium to high loads.

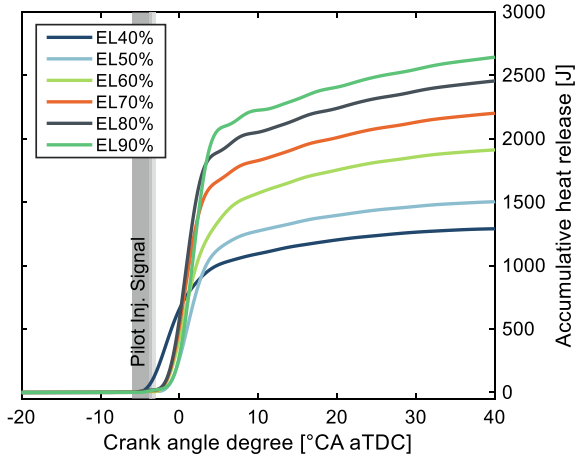

Fig. 10. Accumulative heat released (AccQ) at varying engine loads.

ML32 to ML38.

Overall, we deduce that the composition, trapped mass, and thermal state of the residual gases are the main factors that characterize the reactivity of fresh MeOH-air mixture (pre-flame slow oxidation process), whereby, it influences overall DF combustion. We observe a decline in the performance of MeOH-diesel DF combustion in NVO mode as λ_{MeOH} increases from 3.2 to 3.8. The combustion phasing (CA10, CA50 and CA90) delays, combustion duration increases, AccQ, gIMEP, η_{ind} and η_{comb} are decreased accompanied with increased THC and significantly high CO emissions.

3.5. Effect of engine load

3.5.1. Combustion characteristics

In this test case, the DF combustion is studied to demonstrate the ability of NVO mode to control a wide range of engine operating loads (EL40 – EL90) with an adequate combustion stability, improved emissions, and positive efficiency gains. For this purpose, target-specific performance criteria are set for the experiments including 1) CA50 ≈ 2°CA aTDC, 2) $\eta_{comb} \geqslant 90\%$, 3) $\eta_{ind} \sim 50\%$, and 4) $COV_{IMEP} < 5\%$. The obtained combustion characteristics for the test points from EL40 to EL90 are presented in Figs. 9 - 11. It can be seen that the peak HRR and AccQ increase with an increase in the engine load. In addition, CA50, η_{comb}, η_{ind}, and COV_{IMEP} for the studied test points adequately satisfy the targeted performance criteria. With an increase in the engine load, more MeOH amount is to be injected into the cylinder, which may cause adverse cooling effects on the cylinder temperature and therefore deteriorate the ignition of the in-cylinder mixture. However, based on the insight from the previous sections (Sections 3.2-3.4), several possible parameters are adjusted including λ_{MeOH}, T_{air}, and NVO period, as shown in Table 5. The adjustments of these parameters enabled us to reach the target-specific performance.

Realization of the target-specific performance from the MeOH-diesel DF combustion is a challenging procedure, especially at low-load conditions when a small pilot quantity is utilized. EL40 is operated at the leanest methanol lambda of 4.0 ($\lambda_{MeOH} = 4.0$), which is intrinsically implemented due to the minimum operational limits of the charge-air system. At such lean condition, EL40 requires a high T_{air} of 100 to meet the target limit of η_{comb}. On the other hand, a least amount of residual gases (EVC6 ∼ NVO105) is utilized for EL40, which is necessary to avoid dilution of the in-cylinder mixture. As mentioned earlier in Section 3.2, the DF combustion around TDC_f improves when reactivity (pre-flame slow oxidation processes) of the fresh MeOH-air mixture also improves as a result of increased residual gas amount. However, for EL40 at $\lambda_{MeOH} = 4.0$, a contrary trend is observed i.e., the DF combustion around TDC_f worsens as residual gas amount increases. This is the same combustion behavior described in Section 3.4, when lean mixtures dominate despite a maintained start of combustion timing (an enhanced pre-flame process). This causes a decrease in the overall η_{comb}. Nevertheless, EL40 fairly well satisfies the performance criteria except for CA50, which is purposely adjusted to achieve $\eta_{ind} \sim 50\%$.

Above discussion shows that a certain engine load requires a certain combination of λ_{MeOH}, T_{air}, and amount of residual gases to yield the target-specific combustion characteristics. Therefore, compared to EL40, the T_{air} requirement for EL50 reduces to 80 °C due to increased mixture flammability at richer conditions. It should be noted that when engine load increases at the same NVO period and charge-air quantity, the trapped mass of residuals decreases correspondingly due to higher thermodynamic state (essentially cylinder pressure) of the exhaust gases at EVO. This is also confirmed using the TPA method, as mentioned in Section 2.3.1. For EL50, ∼30 mg lower mass of residuals is estimated at IVC compared to EL40 for the same NVO period and charge-air quantity. Furthermore, the estimated iEGR (Equation 8) values for the test points EL40 – EL90 lie in the range of 20–30%. The validation of the simulated cylinder pressures is presented in Fig. A2 (Appendix A).

At the medium-load range, more residual gases can be utilized with a reduced T_{air}, as also richer conditions can be applied to the fresh MeOH-air mixture. The use of greater amount of residual gases without compromising combustion performance is an advantageous procedure. This is because it allows greater waste heat recovery from the exhaust gases, which consequently results in increased indicated and thermal efficiency. Thus, for EL60 and EL70 at relatively rich conditions and with increased mass of residuals, adapting T_{air} is utilized to meet the performance criteria. However, at high-load conditions, using a greater

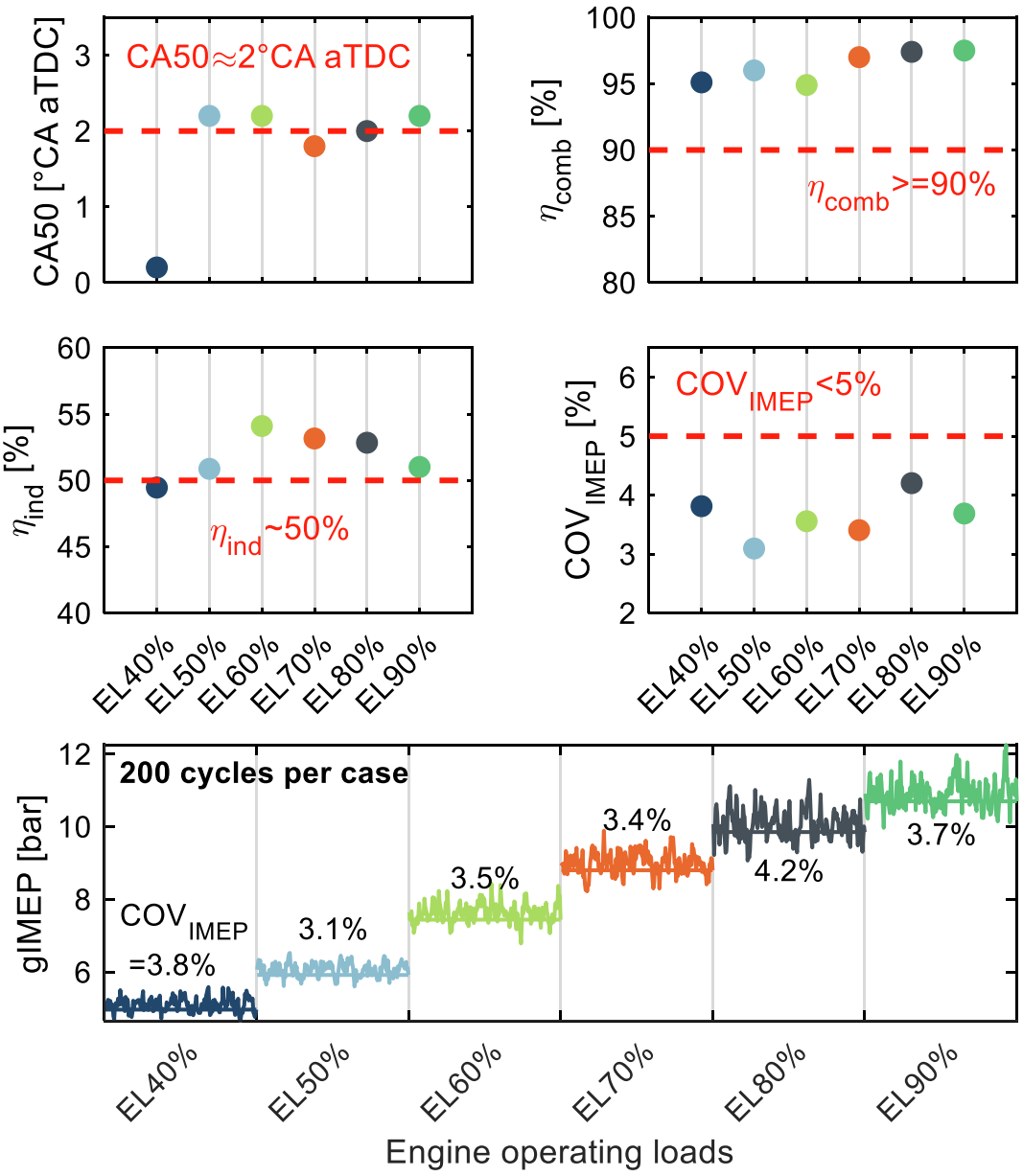

Fig. 11. A minimum set performance criteria and the measured engine performance parameters at varying engine loads.

mass of residuals (longer NVO periods) promotes autoignition and early start of combustion with high pressure-rise rates causing acoustic oscillations. Therefore, in this study, a least mass of residuals with low T_{air} are utilized to control the combustion characteristics of EL80 and EL90. Moreover, high-load conditions are intrinsically operated at richer conditions due to the maximum operating limits of the charge-air system.

From Fig. 11 (as well as Table 5), it can be observed the maximum η_{comb} is reaching to ~ 98% and η_{ind} to ~ 54%. All test points (EL40 – EL90) show η_{comb} and η_{ind} way above the set limits. Interestingly, for such high efficiencies, the DF combustion is reliably controlled (CA50 ~ 2°CA aTDC) and has reasonable combustion stability. Many researchers [47,52,53] have declared COV$_{IMEP}$ = 3–5% as a safe range for engine operations. Here, the studied test points (for gIMEP = 5–11 bar) show COV$_{IMEP}$ below 5%, as estimated over 200 combustion cycles. Overall, we note that the DF combustion in NVO mode is potentially controllable and capable of yielding noticeable high-performance characteristics at a wide range of engine operating loads.

3.5.2. Emission characteristics

Next, we discuss the emission characteristics of the DF combustion at varying engine loads. Fig. 12 presents emission data for the studied test points EL40 – EL90. In NVO mode, the combustion is observed to produce quite low THC, CO, and NO_x emissions despite the challenges associated with low/high load operations, methanol's high octane-number and its latent heat of vaporization. This is because of the hot residual gases from the previous cycle that enhance the overall combustion efficiency, as discussed above. Hot residuals help to increase the reactivity of fresh MeOH-air mixture by possibly commencing pre-flame slow oxidation processes before TDC$_f$. It is worth mentioning that here the molecular weight of THC (containing mostly oxygenated hydrocarbons e.g., formaldehydes) is adjusted for oxygen part so that 50% higher THC emissions could be estimated (also remarked in Section 2.3).

In general, THC and CO are produced due to an incomplete combustion, whereas CO_2 is produced as a result of complete combustion. During a combustion process, NO_x usually forms as thermal NO_x due to locally high in-cylinder temperatures. Therefore, in this study, as more fuel burns completely, more CO_2 and NO_x emissions tend to produce

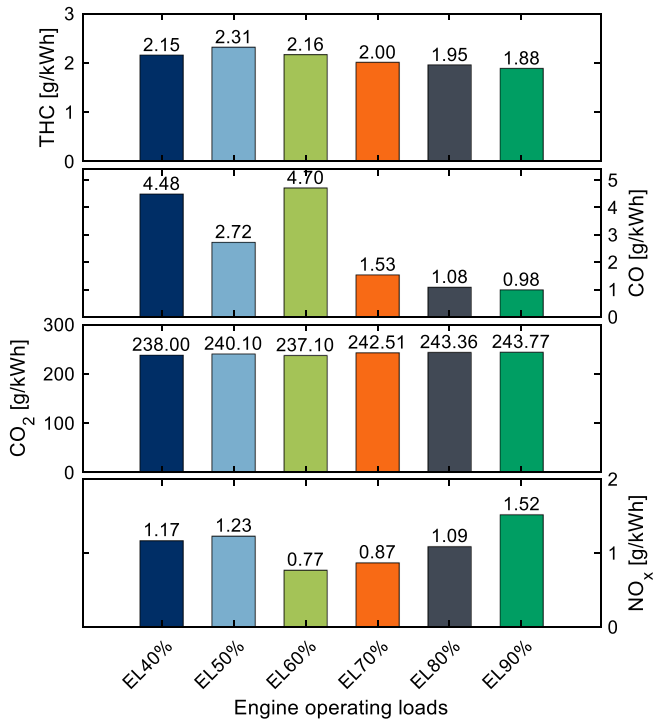

Fig. 12. Indicated specific emission data for varying engine operating loads (EL40 – EL90). The authenticity of the emission values in g/kWh is validated based on the default CO_2 emission factors for diesel and methanol [54]. According to the emission factors, a 10/90 diesel-methanol DF combustion can produce max. ~ 248 g/kWh of CO_2. Thus, here the scale of CO_2 is in good agreement with international reports, showing that the adopted ppm to g/kWh conversion method and the above emission values are credible.

with correspondingly lower THC and CO emissions. THC is regarded as the unburned fuel and CO produces as a result of partial oxidation of the fuel depending on the in-cylinder thermodynamic conditions and combustion mechanisms. For instance, EL60 produces higher CO, however, lower THC, CO_2 and NO_x emissions compared to EL50. This indicates that the slightly lower η_{comb} of EL60 than EL50 is mainly owing to the dilution of the in-cylinder mixture rather than unburned fuel. Apparently, some of the fuel of EL60 was partially oxidized but was not able to fully oxidize to produce higher CO_2 and NO_x compared to EL50. Typically, CO emissions can be reduced by using high T_{air} and richer conditions, as well as avoiding dilution.

In summary, we found here that at a wide range of engine operating loads, the high fractioned MeOH DF combustion in NVO mode can certainly achieve high efficiency targets (η_{ind} ~ 50%) together with low emissions of THC, CO, and NO_x. Additionally, the production of low NO_x emissions despite the high efficiencies is owing to inherent ability of MeOH to burn with low temperatures. Furthermore, in this study, we utilized the AVL smoke meter (using filter paper method according to ISO 10054) to determine filter smoke number (FSN) and soot concentration in the exhaust. We observed no trace of particles or soot on the filter paper left by exhaust gases in all the test points in the present study.

4. Conclusions

In this study, high fractioned (90% on energy base) methanol (MeOH) dual-fuel (DF) combustion is experimentally investigated in a single-cylinder research engine. A constant 10% (energy based) pilot diesel ignites the premixed MeOH-air mixture. Experiments are performed at a constant engine speed of 1500 rpm in the negative-valve overlap (NVO) mode to investigate the effects of varying: 1) NVO period, 2) charge-air temperature (CAT), and 3) methanol lambda (ML), as well as 4) engine load (EL). The combustion at a wide range of engine loads demonstrates the relevance of NVO mode to control and yield high indicated efficiency (η_{ind} ~ 50%) together with low exhaust emissions. Furthermore, 1D GT-power model based on Three Pressure Analysis (TPA) method is adopted to estimate particularly mean mixture temperature and amount of residual gases at the measured engine conditions. The main findings of the present study are concluded in the following.

1) NVO mode enables the use of hot-residual gases from the previous cycle, which facilitate the MeOH-diesel DF combustion to achieve high combustion (η_{comb} > 90%) and indicated (η_{ind} ~ 50%) efficiency more readily than that of the standard valve timing (SVT).
2) Hot residual gases induce a slow pre-flame oxidation processes in the fresh MeOH-air mixture, which generates a pool of reactive species. This increases the reactivity of the in-cylinder mixture to a point that the high-temperature autoignition may occur even earlier than the pilot injection timing. In other words, the slow pre-flame oxidation processes have a direct influence on the reactivity/autoignition of the in-cylinder mixture.
3) The slow pre-flame oxidation processes and the subsequent main combustion are found to be dependent on composition, trapped mass, and thermal state of the residual gases. It is concluded that:
   a. with an increase in the residual gas amount either by increasing the NVO period or methanol lambda (λ_{MeOH}, boost pressure), the slow pre-flame oxidation is possibly always enhancing regardless of the utilized lean conditions. However, there are negative effects on the main combustion above a certain lean-mixture limit.
   b. with an increase in charge-air temperature (T_{air}), both the pre-flame oxidation and the subsequent main combustion are improved.
4) For an engine operating load, a certain combination of NVO period, λ_{MeOH}, and T_{air} helps to yield high efficiency together with low pollutant emissions. For instance, at a wide range of operating loads (gIMEP = 5–11 bar), in general, a η_{comb} of ~ 98% and η_{ind} of ~ 53% is achieved together with low exhaust emissions of THC = 2 g/kWh (despite 50% higher estimate), CO = 2 g/kWh, and NO_x = 1.1 g/kWh.
5) NVO mode helps to maintain high combustion stability despite a high pressure-rise rate at high loads, and ultra-lean conditions at low loads. On average, the coefficient of variability of gIMEP (COV_{IMEP}) is observed to be maintained at low values around 3.5%.

In summary, we observe here that despite the utilization of 90% methanol, the MeOH-diesel DF combustion in NVO mode has the potential to produce high efficiency together with positive environmental impacts. It is believed that with more precise tuning of engine parameters further 0.5–1% efficiency gains can be achieved. On the other hand, the high efficiency gains based on the partial oxidation of methanol in pre-flame regime provide a pathway for further detailed evaluations of interactions between hot residual gases and fresh MeOH. We believe that this pre-flame oxidation process has a close resemblance to the moderate- or -intense low-oxygen dilution (MILD) combustion, generally also known as the flameless combustion.

CRediT authorship contribution statement

Zeeshan Ahmad: Conceptualization, Investigation, Software,

Validation, Methodology, Data curation, Formal analysis, Visualization, Writing – original draft, Writing – review & editing. **Ossi Kaario:** Resources, Supervision, Writing – review & editing. **Cheng Qiang:** Investigation, Validation. **Martti Larmi:** Supervision, Funding acquisition, Writing – review & editing.

Declaration of Competing Interest

The authors declare that they have no known competing financial interests or personal relationships that could have appeared to influence the work reported in this paper.

Acknowledgements

The authors would like to acknowledge the receipt of the following financial support for this research work and authorship. This work was financially supported by Academy of Finland (grant no. 13297248) Fortum-Neste Foundation (grant no. 20200050 and 20210032), and Merenkulun säätiö (grant no. 20210073).

Appendix A

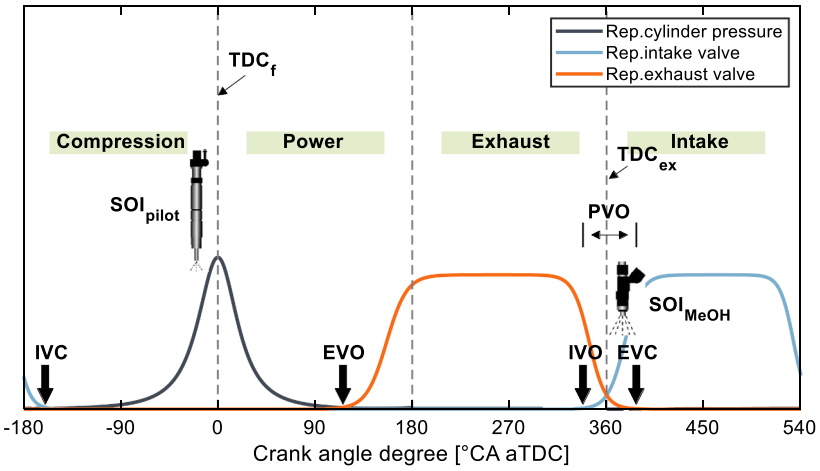

Fig. A1. A schematic illustration of the standard valve timing (SVT) configuration and positive valve overlap (PVO). IVO = 356 °CA aTDC, IVC = -155 °CA aTDC, EVO = 150 °CA aTDC, EVC = 380 °CA aTDC. SOI_{MeOH} = 365 °CA aTDC, SOI_{pilot} = -6 °CA aTDC.

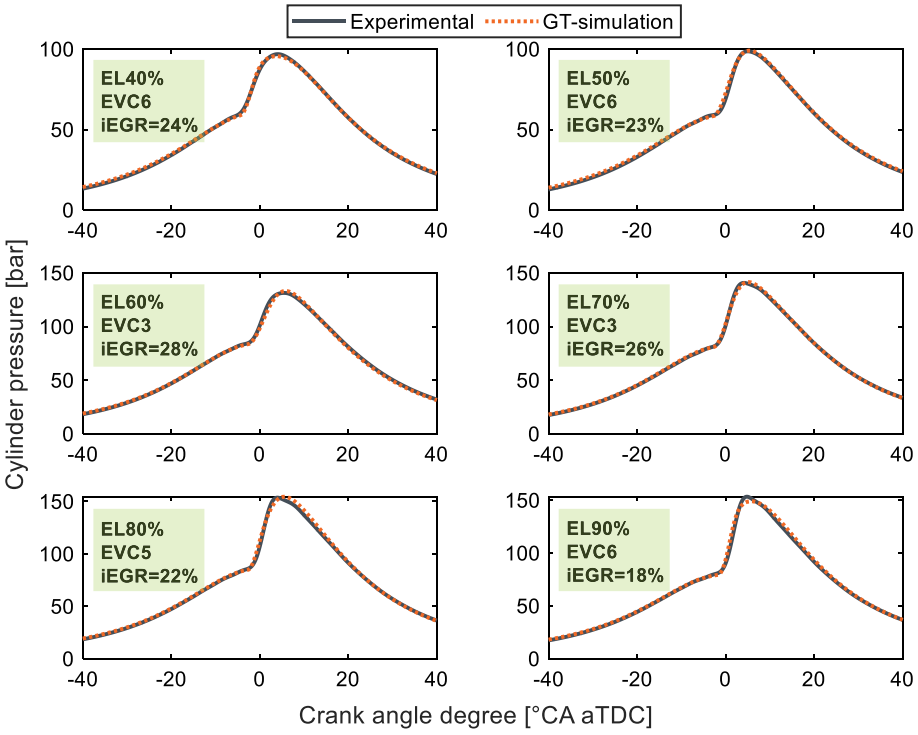

Fig. A2. Validation of GT power model with experimental cylinder pressures to calculate the mass of trapped residuals and the fraction of internal EGR (iEGR) in negative valve overlap (NVO) mode.

References

[1] IEA (2021), Paris, Net Zero by 2050: a roadmap for the global energy sector. https://www.iea.org/reports/net-zero-by-2050, accessed July 12th, 2021.
[2] European commission (EU) – climate action policy, 2050 long-term strategy. https://ec.europa.eu/clima/policies/strategies/2050_en, accessed July 12th, 2021.
[3] IEA (2021), Global EV Outlook 2021. https://www.iea.org/reports/global-ev-outlook-2021, accessed July 12th, 2021.
[4] Gielen D, Boshell F, Saygin D, Bazilian MD, Wagner N, Gorini R. The role of renewable in the global energy transformation. Energy Strategy Rev 2019;1(24):38–50. https://doi.org/10.1016/j.esr.2019.01.006.
[5] Stančin H, Mikulčić H, Wang X, Duić N. A review on alternative fuels in future energy system. Renew Sustain Energy Rev 2020;1(128). https://doi.org/10.1016/j.rser.2020.109927.
[6] Lester MS, Bramstoft R, Münster M. Analysis on electrofuels in future energy systems: a 2050 case study. Energy 2020;15(199). https://doi.org/10.1016/j.energy.2020.117408.
[7] Verhelst S, Turner JW, Sileghem L, Vancoillie J. Methanol as a fuel for internal combustion engines. Prog Energy Combust Sci 2019;1(70):43–88. https://doi.org/10.1016/j.pecs.2018.10.001.
[8] Zhen X, Wang Y. An overview of methanol as an internal combustion engine fuel. Renew Sustain Energy Rev 2015;1(52):477–93. https://doi.org/10.1016/j.rser.2015.07.083.
[9] Izbassarov D, Nyári J, Tekgül B, Laurila E, Kallio T, Santasalo-Aarnio A, et al. A numerical performance study of a fixed-bed reactor for methanol synthesis by CO2 hydrogenation. Int J Hydrogen Energy 2021;46(29):15635–48. https://doi.org/10.1016/j.ijhydene.2021.02.031.
[10] Santasalo-Aarnio A, Nyari J, Wojcieszyk M, Kaario O, Kroyan Y, Magdeldin M, et al. Application of synthetic renewable methanol to power the future propulsion. SAE Technical Paper; 2020 Sep 15. doi: 10.4271/2020-01-2151.
[11] Brinkman ND. Effect of compression ratio on exhaust emissions and performance of a methanol-fueled single-cylinder engine. SAE Technical Paper; 1977 Feb 1. doi: 10.4271/770791.
[12] Jackson MD, Unnasch S, Sullivan C, Renner RA. Transit bus operation with methanol fuel. SAE Trans 1985;94(1):50–61. http://www.jstor.org/stable/44467406.
[13] Pannone GM, Johnson RT. Methanol as a fuel for a lean turbocharged spark ignition engine. SAE Trans 1989;98(1):243–53. http://www.jstor.org/stable/44472027.
[14] Dhaliwal B, Yi N, Checkel D. Emissions effects of alternative fuels in light-duty and heavy-duty vehicles. SAE Technical Paper; 2000 Mar 6. doi: 10.4271/2000-01-0692.
[15] Vancoillie J, Demuynck J, Sileghem L, Van De Ginste M, Verhelst S, Brabant LV, et al. The potential of methanol as a fuel for flex-fuel and dedicated spark-ignition engines. Appl Energy 2013;1(102):140–9. https://doi.org/10.1016/j.apenergy.2012.05.065.
[16] Nguyen DK, Stepman B, Vergote V, Sileghem L, Verhelst S. Combustion Characterization of Methanol in a Lean Burn Direct Injection Spark Ignition (DISI) Engine. SAE Technical Paper; 2019 Apr 2. doi: 10.4271/2019-01-0566.
[17] Hagen DL. Methanol as a fuel: a review with bibliography. SAE Trans 1977;86(1):2764–96. https://www.jstor.org/stable/44644586.
[18] Aakko-Saksa PT, Westerholm M, Pettinen R, Söderström C, Roslund P, Piimäkorpi P, et al. Renewable methanol with ignition improver additive for diesel engines. Energy Fuels 2019;34(1):379–88. https://doi.org/10.1021/acs.energyfuels.9b02654.
[19] Sahoo BB, Sahoo N, Saha UK. Effect of engine parameters and type of gaseous fuel on the performance of dual-fuel gas diesel engines—A critical review. Renew Sustain Energy Rev 2009;13(6–7):1151–84. https://doi.org/10.1016/j.rser.2008.08.003.
[20] Ahmad Z, Kaario O, Qiang C, Larmi M. Effect of pilot fuel properties on lean dual-fuel combustion and emission characteristics in a heavy-duty engine. Appl Energy 2021;15(282). https://doi.org/10.1016/j.apenergy.2020.116134.
[21] Karim GA. Dual-fuel diesel engines. CRC Press; 2015 Mar 2. doi: 10.1201/b18163.
[22] Wang Q, Wei L, Pan W, Yao C. Investigation of operating range in a methanol fumigated diesel engine. Fuel 2015;15(140):164–70. https://doi.org/10.1016/j.fuel.2014.09.067.
[23] Wang B, Yao C, Chen C, Feng J, Lu H, Feng L. To extend the operating range of high MSP with ultra-low emissions for DMDF unit pump engine. Fuel 2018;15(218):295–305. https://doi.org/10.1016/j.fuel.2018.01.028.
[24] Tutak W, Lukacs K, Szwaja S, Bereczky A. Alcohol–diesel fuel combustion in the compression ignition engine. Fuel 2015;15(154):196–206. https://doi.org/10.1016/j.fuel.2015.03.071.
[25] Reitz RD, Duraisamy G. Review of high efficiency and clean reactivity controlled compression ignition (RCCI) combustion in internal combustion engines. Prog Energy Combust Sci 2015;1(46):12–71. https://doi.org/10.1016/j.pecs.2014.05.003.
[26] Paykani A, Garcia A, Shahbakhti M, Rahnama P, Reitz RD. Reactivity controlled compression ignition engine: Pathways towards commercial viability. Appl Energy 2021;15(282). https://doi.org/10.1016/j.apenergy.2020.116174.
[27] Tekgül B, Kahila H, Karimkashi S, Kaario O, Ahmad Z, Lendormy É, et al. Large-eddy simulation of spray assisted dual-fuel ignition under reactivity-controlled dynamic conditions. Fuel 2021;1(293). https://doi.org/10.1016/j.fuel.2021.120295.
[28] Garcia A, Monsalve-Serrano J, Villalta D, Guzman-Mendoza M. Methanol and OMEx as fuel candidates to fulfill the potential EURO VII emissions regulation under dual-mode dual-fuel combustion. Fuel 2021;1(287). https://doi.org/10.1016/j.fuel.2020.119548.
[29] Duraisamy G, Rangasamy M, Nagarajan G. Effect of EGR and premixed mass percentage on cycle to cycle variation of methanol/diesel dual fuel RCCI combustion. SAE Technical Paper; 2019 Jan 9. doi: 10.4271/2019-26-0090.
[30] Jia Z, Denbratt I. Experimental investigation into the combustion characteristics of a methanol-Diesel heavy duty engine operated in RCCI mode. Fuel 2018;15(226):745–53. https://doi.org/10.1016/j.fuel.2018.03.088.
[31] Huang G, Li Z, Zhao W, Zhang Y, Li J, He Z, et al. Effects of fuel injection strategies on combustion and emissions of intelligent charge compression ignition (ICCI) mode fueled with methanol and biodiesel. Fuel 2020;15(274). https://doi.org/10.1016/j.fuel.2020.117851.
[32] Dong Y, Kaario O, Hassan G, Ranta O, Larmi M, Johansson B. High-pressure direct injection of methanol and pilot diesel: a non-premixed dual-fuel engine concept. Fuel 2020;1(277). https://doi.org/10.1016/j.fuel.2020.117932.
[33] Aziz A, Garcia A, Dos Santos CP, Tuner M. Impact of multiple injection strategies on performance and emissions of methanol PPC under low load operation. SAE Technical Paper; 2020 Apr 14. doi: 10.4271/2020-01-0556.
[34] Yao C, Pan W, Yao A. Methanol fumigation in compression-ignition engines: a critical review of recent academic and technological developments. Fuel 2017;1(209):713–32. https://doi.org/10.1016/j.fuel.2017.08.038.
[35] Urushihara T, Hiraya K, Kakuhou A, Itoh T. Expansion of HCCI operating region by the combination of direct fuel injection, negative valve overlap and internal fuel reformation. SAE Trans 2003;112(1):1092–100. http://www.jstor.org/stable/44741337.
[36] Aroonsrisopon T, Nitz DG, Waldman JO, Foster DE, Iida M. A computational analysis of direct fuel injection during the negative valve overlap period in an iso-octane fueled HCCI engine. SAE Technical Paper; 2007 Apr 16. doi: 10.4271/2007-01-0227.
[37] Kuzuoka K, Kondo T, Kudo H, Taniguchi H, Chishima H, Hashimoto K. Controlling combustion with negative valve overlap in a gasoline–diesel dual-fuel compression ignition engine. Int J Engine Res 2016;17(3):354–65. https://doi.org/10.1177/1468087415580216.
[38] Mikulski M, Balakrishnan PR, Hunicz J. Natural gas-diesel reactivity controlled compression ignition with negative valve overlap and in-cylinder fuel reforming. Appl Energy 2019;15(254). https://doi.org/10.1016/j.apenergy.2019.113638.
[39] Pedrozo VB, May I, Lanzanova TD, Zhao H. Potential of internal EGR and throttled operation for low load extension of ethanol–diesel dual-fuel reactivity controlled compression ignition combustion on a heavy-duty engine. Fuel 2016;1(179):391–405. https://doi.org/10.1016/j.fuel.2016.03.090.
[40] Ahmad Z, Kaario O, Karimkashi S, Qiang C, Vuorinen V, Larmi M. Effects of ethane addition on diesel-methane dual-fuel combustion in a heavy-duty engine. Fuel 2021;1(289). https://doi.org/10.1016/j.fuel.2020.119834.
[41] Herranen M, Huhtala K, Vilenius M, Liljenfeldt G. The electro-hydraulic valve actuation (EHVA) for medium speed diesel engines-development steps with simulations and measurements. SAE Technical Paper; 2007 Apr 16. doi: 10.4271/2007-01-1289.
[42] Kaario O, Lendormy E, Sarjovaara T, Larmi M, Rantanen P. In-cylinder flow field of a diesel engine. SAE Technical Paper; 2007 Oct 29. doi: 10.4271/2007-01-4046.
[43] IEA-AMF; Technology collaboration programme on advanced motor fuels, Composition of diesel and gasoline. https://www.iea-amf.org/content/fuel_information/diesel_gasoline/, Accessed May 15th, 2021.
[44] VWR chemicals (supplier), Methanol ≥99.8%, AnalaR, Online specification test results. https://fi.vwr.com/store/catalog/product.jsp?catalog_number=20847.307.
[45] Chen CC, Liaw HJ, Shu CM, Hsieh YC. Autoignition temperature data for methanol, ethanol, propanol, 2-butanol, 1-butanol, and 2-methyl-2, 4-pentanediol. J Chem Eng Data 2010;55(11):5059–64. https://doi.org/10.1021/je100619p.
[46] Sarjovaara T, Larmi M, Vuorinen V. Effect of charge air temperature on E85 dual-fuel diesel combustion. Fuel. 2015 Aug 1;153:6-12. doi: 10.1016/j.fuel.2015.02.096.
[47] Heywood JB. Internal combustion engine fundamentals. McGraw-Hill Education; 2018. https://www.accessengineeringlibrary.com/content/book/9781260116106.
[48] Sandstroem-Dahl C, Erlandsson L, Gasste J, Lindgren M. Measurement methodologies for hydrocarbons, ethanol and aldehyde emissions from ethanol fuelled vehicles. SAE International Journal of Fuels and Lubricants 3(2). 2010 Jan 1;3(2):453-66. http://www.jstor.org/stable/26272951.
[49] Cylinder pressure analysis; Relevant publications, use of TPA (three pressure analysis). https://www.gtisoft.com/wp-content/uploads/publication/BMW_ThreePressureAnalysis.pdf, Accessed July 20th, 2021.
[50] Rodriguez JF, Cheng WK. Potential of negative valve overlap for part-load efficiency improvement in gasoline engines. SAE Int J Engines 2018;11(6):657–68. https://www.jstor.org/stable/26649122.
[51] Aniolek KW, Wilk RD. Preflame oxidation characteristics of methanol. Energy Fuels 1995;9(3):395–405. https://pubs.acs.org/doi/pdf/10.1021/ef00051a002.
[52] Maurya RK, Agarwal AK. Statistical analysis of the cyclic variations of heat release parameters in HCCI combustion of methanol and gasoline. Appl Energy 2012;89(1):228–36. https://doi.org/10.1016/j.apenergy.2011.07.002.
[53] Zhang HG, Han XJ, Yao BF, Li GX. Study on the effect of engine operation parameters on cyclic combustion variations and correlation coefficient between the pressure-related parameters of a CNG engine. Appl Energy 2013;1(104):992–1002. https://doi.org/10.1016/j.apenergy.2012.11.043.
[54] Emission factors for greenhouse gas inventories, Mobile combustion CO2 emission factors, 2014. https://www.epa.gov/sites/default/files/2015-07/documents/emission-factors_2014.pdf, Accessed August 2nd, 2021.